Effects of Growth Month Variations on Volatile Profiles, Anti-Glycation Capacity, and Antioxidant Activity of *Cyclocarya paliurus* Leaves: A SPME-GC-MS Study

Yanmeng Fu , Qiyue Shao , Liang Chen , Tianxiao Zhang , Jingyi Zhao , Wenhui Zhou , Bin Long , Dai Lu , Wei Wang , Xing Tian *

Posted Date: 13 February 2026

doi: 10.20944/preprints202602.1111.v1

Keywords: *Cyclocarya paliurus* leaves; volatile compounds; anti-glycation capacity; antioxidant activity; SPME-GC-MS

 doi:10.20944/preprints202602.1111.v1

Article

Effects of Growth Month Variations on Volatile Profiles, Anti-Glycation Capacity, and Antioxidant Activity of *Cyclocarya paliurus* Leaves: A SPME-GC-MS Study[1]

Yanmeng Fu [1,†], Qiyue Shao [1,†], Liang Chen [1,2], Tianxiao Zhang [1], Jingyi Zhao [1], Wenhui Zhou [1], Bin Long [1], Dai Lu [1,3,4], Wei Wang [1] and Xing Tian [1,3,4,*]

[1] TCM and Ethnomedicine Innovation & Development International Laboratory, Innovative Material Medical Research Institute, School of Pharmacy, Hunan University of Chinese Medicine, Changsha, 410208, China

[2] School of Food Science and Technology, Jiangnan University, 1800 Lihu Road, Wuxi 214122, China

[3] Department of Food and Drug Engineering, School of Pharmacy, Hunan University of Chinese Medicine, Changsha, Hunan 410208, China

[4] Hunan Engineering and Technology Research Center for Health Products and Life Science, Changsha 410208, China

* Correspondence: acctianxing@hotmail.com; Tel.: +86-73188458331

† Yanmeng Feng and Qiyue Shao contributed equally.

Abstract

Cyclocarya paliurus leaves are widely consumed as "sweet tea", yet mature leaves harvested after spring remain underutilized despite their potential health-promoting value. This study aimed to clarify how harvest month modulates volatile signatures and functional bioactivities of *C. paliurus* leaves across the growing season. Leaves collected from May to September (Q5–Q9) were extracted with water and characterized by spectrophotometric quantification of major non-volatile constituents (TPC, TFC, TP, and TSC), SPME–GC–MS profiling of volatile organic compounds (VOCs), DPPH radical scavenging assays, and BSA-based glucose/fructose glycation models; multivariate and correlation analyses were further applied to link chemical dynamics with bioactivities. Antioxidant capacity exhibited clear harvest-stage dependence, with Q9 and Q6 showing the strongest DPPH scavenging and the lowest IC_{50} values (0.119 and 0.222 mg/mL, respectively). Anti-glycation activity displayed a similar temporal pattern: in both Glu–BSA and Fru–BSA systems, Q6 and Q9 consistently achieved the most pronounced inhibition of AGEs accumulation, exceeding 70% at weeks 3–4. VOCs underwent substantial seasonal remodeling, characterized by alkene predominance in Q6 (74.00%), alcohol enrichment in Q7 (38.90%), and a transient increase of alkanes in Q8 (22.32%), with ketones recurring at early and late stages. Correlation analysis and a three-phase schematic model collectively suggest that functional differentiation is driven by coordinated interactions between the non-volatile matrix (notably flavonoids) and stage-specific volatile signatures (e.g., alkenes and ketones). Overall, these findings provide a mechanistic basis for precision harvesting and stage-targeted utilization of mature *C. paliurus* leaves to optimize both bioactivity and aroma quality.

Keywords: *Cyclocarya paliurus* leaves; volatile compounds; anti-glycation capacity; antioxidant activity; SPME-GC-MS

Solid-Phase Microextraction (SPME) ; Gas chromatography-mass spectrometry (GC–MS) ; Liquid chromatography-mass spectrometry (LC-MS); Volatile organic compounds (VOCs); Partial least square regression (PLSR); Bovine serum albumin (BSA); O-phenylenediamine (OPD); Phosphate buffer saline (PBS); 1,1-diphenyl-2-picrylhydrazyl (DPPH); Total Phenolic Content (TPC); Total Flavonoid Content (TFC); Total Polysaccharide (TP) Content; Total Saponin Content (TSC); Electrospray ionization (ESI); Principal component analysis (PCA); Advanced glycation end-products (AGEs); Electron ionization (EI)

 doi:10.20944/preprints202602.1111.v1

1. Introduction

Cyclocarya paliurus (Batalin) Iljinskaja (*C. paliurus*), also known as the sweet tea tree, is a deciduous tree belonging to the genus *Cyclocarya* of the family Juglandaceae and is one of the endemic plant resources in China, mainly distributed in the middle and lower reaches of the Yangtze River [1]. Due to their inherent sweetness, *C. paliurus l*eaves have been traditionally utilized as a "sweet tea" in folk medicine, with a long history of use and a well-established safety profiles[2]. On October 30, 2013, *C. paliurus* leaves were officially approved in China as a novel food ingredient and permitted for consumption as a conventional food in the form of infusion[3]. Currently, functional tea products derived from the immature leaves of *C. paliurus* have achieved large-scale industrialization. Notably, this species represents the first Chinese herbal tea to receive approval from the U.S. Food and Drug Administration (FDA), highlighting its significant market potential and international recognition[4]. Despite the established industry, current production primarily focuses on the tender leaves harvested in April. Consequently, a substantial volume of mature leaves from subsequent growth stages remains underutilized, leading to a significant waste of potential resources. In fact, previous studies have demonstrated that the mature leaves of *C. paliurus* possess potential health-promoting properties, including hypoglycemic, hypolipidemic, and anti-aging effects, thereby suggesting promising prospects for their further high-value applications[5]. Therefore, with the increasing attention to the edible and health-promoting values of *C. paliurus*, its chemical composition and biological activities have gradually become research hotspots.

In recent years, with the increasing attentio*n to C. paliurus* in the development of functional foods and natural plant resources, studies on its chemical composition and biological activities have been continuously growing. A large body of evidence indicates that *C. paliurus* leaves are rich in various bioactive constituents, including flavonoids and their glycosides, polyphenols, phenolic acids, alkaloids, triterpenoids, and polysaccharides, which collectively constitute the material basis for their antioxidant and anti-glycation activities[6–8]. In terms of antioxidant capacity, numerous studies utilizing various in vitro assays, such as DPPH, ABTS, FRAP, and models for hydroxyl and superoxide anion radical scavenging have confirmed that *C. paliurus* leaves extracts exhibit potent radical scavenging capabilities and significant total antioxidant activity[9,10]. Further animal experiments have demonstrated that *C. paliurus* can significantly enhance the activities of endogenous antioxidant enzymes, including superoxide dismutase (SOD), catalase (CAT), and glutathione peroxidase (GSH-Px), while reducing lipid peroxidation levels, thereby exerting protective effects against oxidative stress related damage in the liver, pancreas, and kidneys[11,12]. Regarding anti-glycation and hypoglycemic effects, component isolation and in vivo studies have shown that the flavonoid and polysaccharide fractions are the main contributors to the antihyperglycemic activity of *C. paliurus* leaves[13]. Studies based on type 2 diabetic animal models induced by streptozotocin (STZ) or by a high-fat diet combined with low-dose STZ further revealed that *C. paliurus* leaves extracts significantly reduce fasting blood glucose levels, improve glucose tolerance and insulin sensitivity, and exert hypoglycemic and pancreatic protective effects by inhibiting pancreatic β-cell apoptosis and maintaining islet structural integritys[14–16]. Meanwhile, studies on diabetic complications have gradually emerged, indicating that *C. paliurus* can confer protection against diabetic nephropathy and related complications by inhibiting aldose reductase activity and alleviating oxidative stress[17].

With regard to volatile constituents, the application of advanced analytical techniques, such as HS-SPME-GC-MS（Headspace-Solid-Phase-Microextraction-Gas Chromatography-Mass Spectrometry）, HS-GC-IMS (Headspace - Gas Chromatography - Ion Mobility Spectrometry), has facilitated the detailed characterization of the volatile composition of *C. paliurus* leaves. These studies have identified the primary volatile compounds, which predominantly include alcohols, aldehydes, ketones, esters, olefins, and terpenoids, collectively contributing to the characteristic aroma profile of *C. paliurus* tea[18–20]. From the dual perspectives of leaf ontogeny and metabolic regulation, existing literature demonstrates that the concentrations of flavonoids, phenolic acids, alkaloids, and terpenoids in *C. paliurus* leaves do not remain static during growth. Instead, these secondary

 doi:10.20944/preprints202602.1111.v1

metabolites undergo dynamic flux facilitated by a series of continuous biochemical transformations, including degradation, methylation, glycosylation, redox reactions, and isomerization[21]. Consequently, significant differences in metabolic intensity and pathways occur at different growth stages, leading to stage-dependent changes in chemical composition and biological activities. This dynamic variation not only modulates the accumulation and biotransformation of non-volatile bioactive constituents (such as flavonoids, polyphenols, and glycosides), but may also govern the biosynthesis and emission of volatile compounds via precursor conversion and metabolically coupled pathways.

Collectively, contemporary research on *C. paliurus* has evolved from the fundamental identification of chemical constituents to comprehensive functional characterizations, including antioxidant activity, hypoglycemic effects, and metabolic regulation. Concurrent advancements have also been documented in the profiling of volatile organic compounds (VOCs). However, existing literature primarily emphasizes comparative analyses across disparate geographical origins or bioactivity assessments of samples harvested at a single time point. Systematic investigations concerning the coordinated dynamic fluctuations in volatile profiles, antioxidant capacity, and anti-glycation potential throughout the growth cycle or across different leaf ages remain significantly underrepresented.

Therefore, this study systematically characterized *C. paliurus* leaves harvested between May and September to investigate the month-dependent fluctuations in volatile profiles, as well as their antioxidant and anti-glycation activities. The concentrations of total phenolics (TPC), total flavonoids (TFC), total polysaccharides (TP), and total saponins (TSC) were quantified using established spectrophotometric protocols, specifically the Folin–Ciocalteu assay, aluminum chloride ($AlCl_3$) colorimetry, the phenol-sulfuric acid method, and the vanillin-perchloric acid method, respectively. And the volatile organic compounds (VOCs) were identified and semi-quantitated via solid-phase microextraction coupled with gas chromatography-mass spectrometry (SPME-GC-MS) to delineate temporal aroma signatures. Furthermore, in vitro antioxidant capacity was determined through DPPH radical scavenging assays, while anti-glycation potential was rigorously assessed using a bovine serum albumin (BSA) glycation model. By establishing correlations between the dynamic evolution of volatile constituents and their biological activities, this research elucidates the functional material basis of *C. paliurus* leaves across different ontogenetic stages, providing a scientific foundation for the high-value utilization of mature leaf resources.

2. Materials and Methods

2.1. Reagents and Chemicals

C. paliurus leaves samples collected at different growth stages were obtained from Hunan Yueling Junshan Agroforestry Technology Co., Ltd. (Hunan, China). Folin–Ciocalteu phenol reagent was purchased from Hefei Bomei Biotechnology Co., Ltd. (Hefei, China). Anhydrous ethanol was supplied by Anhui Ante Food Co., Ltd. (Anhui, China), while phenol was obtained from Guangdong Guanghua Technology Co., Ltd. (Guangdong, China). Sulfuric acid and perchloric acid were purchased from Hunan Huihong Reagent Co., Ltd. (Hunan, China). The following guaranteed reagents were provided by Chengdu Lemeitian Pharmaceutical Technology Co., Ltd. (Chengdu, China): gallic acid, rutin solution, glucose, fructose, methylglyoxal (MGO; 40% aqueous solution), bovine serum albumin (BSA), o-phenylenediamine (OPD), hydrochloric acid, phosphate buffer saline (PBS), 2,2-diphenyl-1-picrylhydrazyl (DPPH), β-mercaptoethanol, NaHCO3, Tris and oleanolic acid. Anhydrous sodium carbonate, sodium nitrite, aluminum nitrate, vanillin, and glacial acetic acid were purchased from Sinopharm Chemical Reagent Co., Ltd. (Shanghai, China).

 doi:10.20944/preprints202602.1111.v1

2.2. Preparation of C. paliurus Leaves Sample

All *C. paliurus* leaves samples were collected from Huping Mountain, Shimen County, Hunan Province, P.R. China (110.773665° N, 29.94036696° E). To elucidate the accumulation dynamics of leaf constituents over the growing season, approximately 200 ± 0.50 g of fresh, fully expanded and mature leaves were sampled at four-week intervals during the 2024 growing period (3 May, 1 June, 3 July, 6 August, and 1 September). For each sampling time point, leaves were randomly harvested from three trees exhibiting comparable canopy characteristics and pooled to generate a representative composite sample. All collected samples were oven-dried at 60 °C to constant weight, finely ground into powder, and stored at −20 °C until subsequent analysis.

2.3. Extraction C. paliurus Leaves Samples

Each powdered sample of *C. paliurus* leaves (6.0 ± 0.01 g) was extracted with 120 mL of distilled water in a 250 mL round-bottomed flask at 90 °C for 40 min using a water bath. The extract was then centrifuged at 4,500 rpm for 5 min at 4 °C. The supernatant was filtered successively through three layers of gauze three times. The combined filtrate was concentrated under reduced pressure (75 kPa) at 65 °C, followed by lyophilization in a freeze-dryer (Xinzhi Freeze-drying Equipment Co., Ltd., Ningbo, China). The resulting lyophilized powder was sealed and stored at −20 °C until subsequent analysis.

2.4. Determination of Total Phenolic Content (TPC), Total Flavonoid Content (TFC), Total Polysaccharide Content (TP) and Total Saponin Content (TSC)

Lyophilized *C. paliurus* leaves powder was used for the determination of total phenolic content (TPC), total flavonoid content (TFC), total polysaccharide content (TP), and total saponin content (TSC). Extraction yield was calculated as the percentage ratio of the final lyophilized dry mass to the initial fresh mass. All constituent contents were expressed on a dry weight basis of the lyophilized powder.

The total phenolic content (TPC) of lyophilized *C. paliurus* leaves powder was determined using the Folin–Ciocalteu colorimetric method, as previously described by Xiao et al. [22]. Quantification was performed using a gallic acid calibration curve, and results were expressed as milligrams of gallic acid equivalents per gram of dry weight (mg GAE/g DW). The total flavonoid content (TFC) was measured by the aluminum nitrate colorimetric method according to Yang et al. [23]. A rutin standard curve was employed for calibration, and the results were reported as milligrams of rutin equivalents per gram of dry weight (mg RE/g DW). The total polysaccharide content (TP) was determined using the phenol–sulfuric acid method [24], with glucose used as the reference standard. Data were expressed as milligrams of glucose equivalents per gram of dry weight (mg GE/g DW). The total saponin content (TSC) was quantified following the spectrophotometric method described by de Aguiar et al. [25], which involves acid hydrolysis to release triterpene aglycones, followed by vanillin-based color development. Quantification was based on an oleanolic acid standard curve, and results were expressed as milligrams of oleanolic acid equivalents per gram of dry weight (mg OAE/g DW).

2.5. Antioxidant Evaluation of C. paliurus Leaves Extracts (DPPH Test)

A methanolic solution of DPPH (0.315 mM) was freshly prepared prior to analysis. *C. paliurus* extracts were serially diluted (20–200-fold) to obtain final concentrations of 0.2, 0.5, 1.0, 2.0, 3.5, and 5.0 mg/mL. For the assay, 20 μL of each diluted sample was mixed with 200 μL of the DPPH solution in disposable optical polystyrene 96-well plates.[26]. The reaction mixture was incubated at room temperature in the dark for 30 min, after which the absorbance was measured at 517 nm using a microplate spectrophotometer. All measurements were performed in triplicate. The free radical scavenging activity was inversely proportional to the absorbance value. The scavenging activity (%) was calculated using the following equation:[27]:

 doi:10.20944/preprints202602.1111.v1

$$Inhibition(\%) = \frac{ABS_{control} - (ABS_{sample} - ABS_{blank})}{ABS_{control}} \times 100$$

ABScontrol: Absorbance of the 220 μL DPPH-methanol solution in methanol,

ABSsample: Absorbance of the 20 μ L sample solutions (various concentrations) + 200 μ L DPPH-methanol solution,

ABSblank: Absorbance of the 220 μ L sample solutions (various concentrations).

2.6. Antiglycative Evaluation of C. paliurus leaves Extracts in BSA Models

To evaluate the antiglycation activity of *C. paliurus* leaves extracts, two in vitro glycation models, namely glucose–BSA (Glu–BSA) and fructose–BSA (Fru–BSA), were established. For the Glu–BSA model, bovine serum albumin (BSA; 50 mg mL^{-1}) and *d*-glucose (0.8 M) were dissolved in 100 mL of phosphate-buffered saline (PBS), corresponding to 5 g BSA and 14.4 g glucose. The Fru–BSA model was prepared in an analogous manner by dissolving 5 g BSA and 45.05 g fructose in 100 mL PBS to obtain final concentrations of 50 mg mL^{-1} BSA and 2.5 M fructose. For each glycation system, 1 mL of the reaction mixture was combined with 50 μL of the test extract. Control samples were prepared by adding 50 μL of methanol in place of the extract. Sodium azide (NaN_3) was added to all samples at a final concentration of 0.2 g L^{-1} to prevent microbial contamination. The reaction mixtures were incubated at 37 °C for 4 weeks.The formation of advanced glycation end-products (AGEs) was monitored weekly by measuring fluorescence intensity. At each time point, 200 μL of the reaction mixture was transferred to a black 96-well microplate, and fluorescence was recorded using a Victor X4 Multilabel Plate Reader (PerkinElmer, USA) at excitation and emission wavelengths of 330 nm and 410 nm, respectively. The fold change in AGEs-associated fluorescence for each extract was calculated according to Equation A, and the corresponding AGEs inhibition rate was determined using Equation B. [28].

$$\text{A: } \mathrm{Re}\,lativeAGE_s fluorescence = \frac{Trt_n}{Ctl_0}$$

$$\text{B: } inhibition(\%) = \left(1 - \frac{Trt_n}{Ctl_0}\right) \times 100$$

Trt n: The fluorescence of a solution with *C. paliurus* extract at the n wk;

Ctl 0: The original fluorescence of a corresponded control solution;

Ctl n: The fluorescence of a corresponded control solution at the n wk.

2.7. Gas Chromatography Mass Spectrometry (GC-MS) Analysis

Approximately 0.50 ± 0.01 g of the sample was accurately weighed into a 15 mL headspace vial and equilibrated in a thermostatic water bath at 60 °C for 10 min. A preconditioned solid-phase microextraction (SPME) fiber (250 °C for 30 min) was then introduced into the vial for headspace extraction, with adsorption allowed to proceed for 45 min. Immediately after extraction, the SPME fiber was inserted into the GC injector port and thermally desorbed at 250 °C for 3 min, during which time data acquisition was initiated.

GC conditions: A DB-5MS capillary column (30 m × 0.25 mm, 0.25 μ m) was employed. The carrier gas was high-purity helium (purity ≥ 99.999%) under constant flow mode at a flow rate of 1.7 mL/min. The injection port temperature was set at 250°C in splitless mode. The temperature program was as follows: initial temperature 40°C, held for 5 min; increased to 85 °C at 10°C/min, held for 3 min; then raised to 200°C at 4 °C/min, held for 3 min; finally increased to 230°C at 10°C/min, held for 1 min.

MS conditions: Electron ionization (EI) source was used with an ionization energy of 70 eV. The ion source temperature was 200 °C, the transfer line temperature was 250 °C, and the quadrupole temperature was 150 °C. Full scan mode was applied with a mass scan range of m/z 35–400 amu. The solvent delay time was 3 min, emission current was 100 μ A, and detector voltage was 1.4 kV. The

 doi:10.20944/preprints202602.1111.v1

NIST 14 mass spectral library was utilized for compound identification, and compounds with a match factor >80% were retained. Each sample was analyzed in triplicate to ensure the reproducibility and reliability of the results [29].

2.8. Statistical Analysis

The taste attributes obtained via electronic tongue analyses are expressed as means ± standard deviation (SD) and was subjected to a one-way analysis of variance (ANOVA) with Duncan's test using SPSS (25.0, IBM) software. Hierarchical clustering analysis was performed using TBtools software (TB tools, Guangzhou, China), while SIMCA-P 14.1 multivariate statistical software (Umetrics, Umea, Sweden) was used for generating radar plots, principal component analysis (PCA), and orthogonal partial least squares discriminant analysis (OPLS-DA) along with other visual representations.

3. Results

3.1. Changes in TPC, TFC, TP and TSC of C. Paliurus Leaves in Different Growth Periods

The contents of total phenolics (TPC), total flavonoids (TFC), total saponins (TSC), and total protein (TP) in *C. paliurus* leaves exhibited distinct growth stage–dependent variation patterns (Figure 1). Among these components, TPC remained relatively stable from Q5 to Q9, showing only minor fluctuations, indicating that phenolic accumulation was largely maintained throughout the main growing season with minimal dilution effects from leaf expansion. In contrast, The TFC displayed pronounced temporal variation, increasing markedly from Q5 to reach a maximum at Q7, remaining at a relatively high level at Q8, and then decreasing sharply at Q9. This trend suggests that flavonoid biosynthesis is strongly influenced by developmental stage and seasonal environmental conditions, such as increased irradiance and temperature during active growth. Similar mid-summer peaks in flavonoid accumulation have been reported for *C. paliurus* and are supported by recent metabolomics studies showing substantial seasonal variation in secondary metabolites [1,30,31]. Compared with the TFC, TSC exhibited relatively limited variation across the growth stages, with only a modest increase at Q7, implying a more tightly regulated biosynthesis or slower metabolic turnover of saponins. TP showed a distinct V-shaped pattern, decreasing from Q5 to a minimum at Q6 and subsequently increasing toward Q9. The early decrease may be associated with rapid leaf expansion–induced dilution, whereas the later increase likely reflects enhanced protein synthesis or a concentration effect at later developmental stages.In general, TFC and TP showed greater seasonal variability than TPC and TSC, indicating that flavonoids and proteins are the most growth stage–responsive constituents in C. paliurus leaves and may therefore play key roles in determining their functional and nutritional properties.

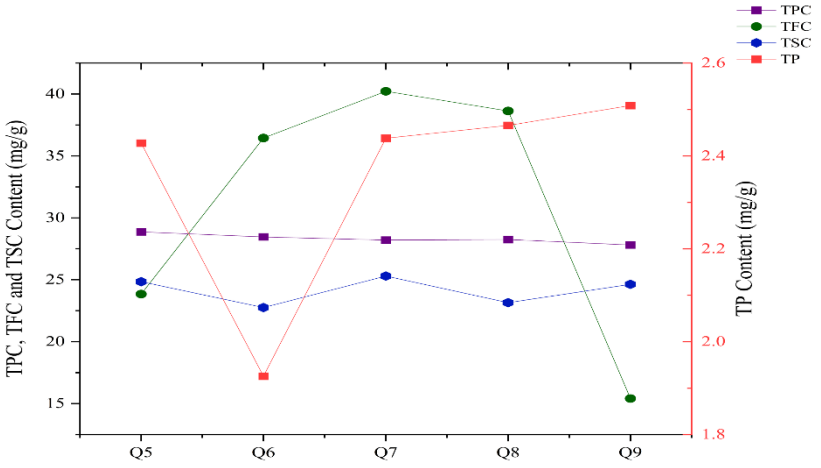

 doi:10.20944/preprints202602.1111.v1

Figure 1. Changes in the TPC, TFC, TSC, and TP of *C. paliurus* leaves in five different months Notes: TPC (Total Phenolic Content), TFC (Total Flavonoid Content), TP (Total Polysaccharide Content), and TSC (Total Saponin Content). Q5-Q9 refers to the samples of the leaves of C. paliurus collected from May to September.

3.2. Changes of Antioxidant Activity

The DPPH radical scavenging activity of *C. paliurus* leaves extracts increased in a concentration-dependent manner for all sampling months (Figure 2), demonstrating typical dose–response behavior. However, marked differences in antioxidant capacity were observed among growth periods. Extracts from Q9 and Q6 exhibited substantially stronger scavenging activity than those from other months across the tested concentration range. At 5 mg/mL, the scavenging rates of Q6 and Q9 exceeded 80%, approaching that of the positive control (vitamin C), whereas Q5, Q7, and Q8 showed relatively weaker activities. These differences were further confirmed by IC50 values (Table 1), with Q9 showing the lowest IC50 (0.119 mg/mL), followed by Q6 (0.222 mg/mL), indicating superior antioxidant capacity at later and mid-growth stages. The weaker antioxidant performance of Q5 may be related to the incomplete development of secondary metabolism at early growth stages. Notably, the strong antioxidant activity of Q6 and Q9 was not directly correlated with TP content, suggesting that proteins are not the primary contributors to DPPH scavenging activity.Recent research suggests that the antioxidant capacity of C. paliurus is often the result of a synergistic effect between flavonoids and water-soluble polysaccharides, rather than a single component [32,33]. Instead, the enhanced antioxidant capacity observed at mid-to-late growth stages is more likely associated with flavonoids and other phenolic-derived compounds, which possess multiple hydroxyl groups capable of donating electrons or hydrogen atoms to neutralize free radicals[**Error! Reference source not found.**]. The discrepancy in scavenging behavior between Q7 and Q8, despite comparable IC50 values, further implies that qualitative differences in antioxidant composition, rather than total content alone, may influence radical scavenging efficiency.

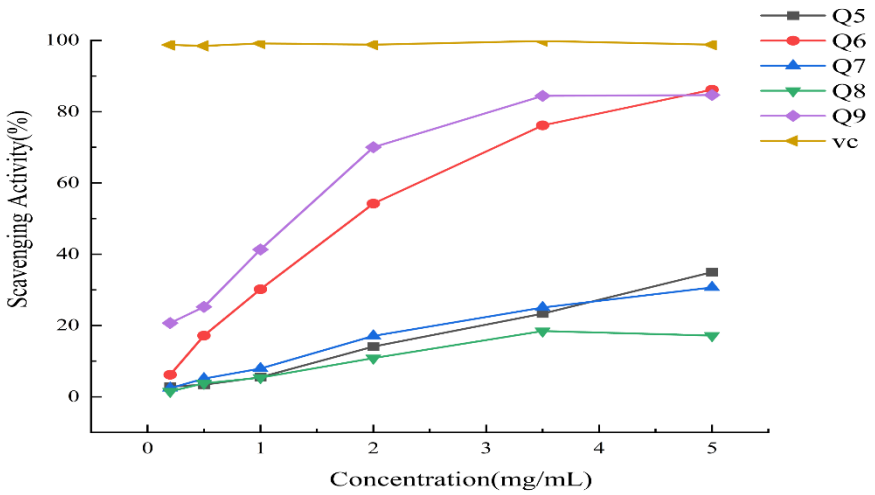

Figure 2. Scavenging ability against DPPH of *C. paliurus* leaves in five different months. Notes: vc refers to vitamin C); Q5-Q9 refers to the samples of the leaves of C. paliurus collected from May to September.

Table 1. IC50 values of DPPH free radical scavenging capacity of *C. paliurus* in five different months.

Month	IC_{50}(DPPH·)
Q5	0.297
Q6	0.222
Q7	0.252
Q8	0.242
Q9	0.119

 doi:10.20944/preprints202602.1111.v1

3.3. Changes of Anti-Glycation Capacity

The anti-glycation activity of C. paliurus leaf extracts was evaluated using both Glu-BSA and Fru-BSA models over prolonged incubation (Figure 3). In both models, the fluorescence intensity of AGEs in the control groups increased steadily with incubation time, confirming the progressive formation of glycation end products. In contrast, all leaf extracts suppressed AGEs accumulation to varying extents, with clear differences among growth periods.In the Glu-BSA system, extracts from Q6 and Q9 consistently exhibited lower AGEs fluorescence intensity after week 2 compared with other months, indicating stronger inhibition of glycation reactions. Similar trends were observed in the Fru-BSA model, where Q9 showed the most pronounced suppression of AGEs formation during weeks 2–4, followed by Q6. These observations were further supported by AGEs inhibition rates, which increased markedly at later incubation stages. In both models, Q6 and Q9 achieved the highest inhibition rates (>70%) at weeks 3–4, whereas Q5, Q7, and Q8 showed comparatively weaker effects. The superior anti-glycation performance of Q9 extracts suggests that bioactive compounds involved in glycation inhibition preferentially accumulate at later growth stages. This is supported by recent metabolomic and transcriptomic analyses, which identified September (late growth stage) as a critical period for the biosynthesis of hypoglycemic and functional metabolites in *C. paliurus* leaves [35,36].

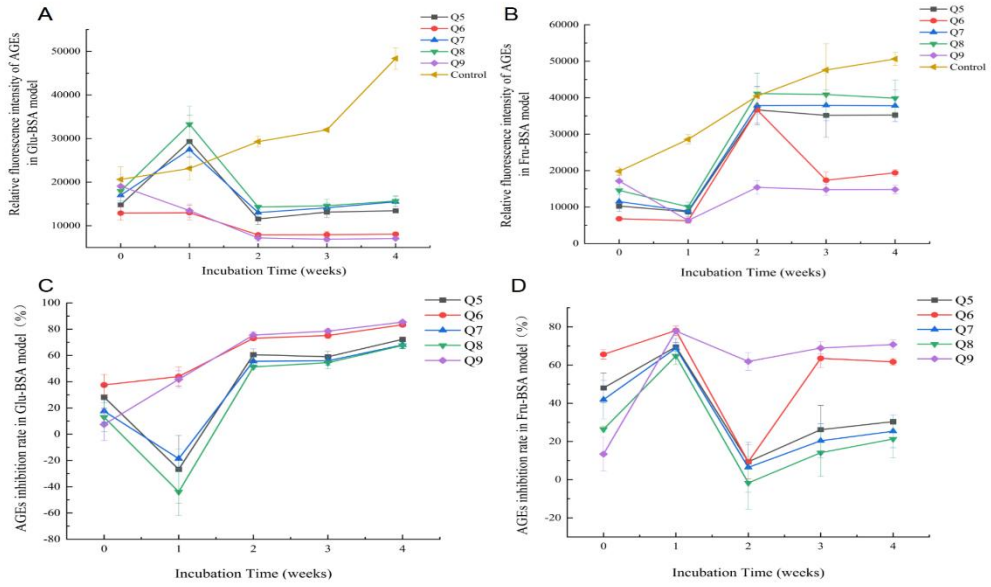

Figure 3. The anti-glycation potential of different monthly C. paliurus leaves under long-term incubation. (A) Relative fluorescence intensity of AGEs in Glu-BSA model; (B) Relative fluorescence intensity of AGEs in Fru-BSA model; (C) AGEs inhibition rate in Glu-BSA model; (D) AGEs inhibition rate in Fru-BSA model. Glu-BSA model: glucose-bovine serum albumin model; Fru-BSA model: fructose-bovine serum albumin model; AGEs: advanced glycation end products； Q5-Q9 refers to the samples of the leaves of C. paliurus collected from May to September.

This trend is in agreement with the enhanced antioxidant activity, further supporting the premise that antioxidant mechanisms, particularly the scavenging of reactive oxygen species and the sequestration of reactive carbonyl intermediates, play critical roles in inhibiting the formation of advanced glycation end-products (AGEs). Antioxidants can interfere with multiple stages of the glycation cascade, thereby limiting both oxidative and carbonyl stress associated with AGEs generation. Moreover, the distinct responses observed between the glucose–BSA (Glu–BSA) and fructose–BSA (Fru–BSA) models suggest that differences in extract composition may differentially modulate sugar-specific glycation pathways. Fructose is known to exhibit higher glycation reactivity than glucose due to its greater proportion of open-chain structures, leading to more rapid and severe AGEs formation. The comparatively stronger inhibitory effects observed in one model over the other

 doi:10.20944/preprints202602.1111.v1

therefore imply that specific bioactive constituents in *C. paliurus* extracts may preferentially target fructose- or glucose-mediated glycation reactions.Furthermore, the studies on polysaccharide synthesis have also highlighted the contribution of late-stage macromolecules to the overall bioactivity of the leaves [**Error! Reference source not found.**]. On the whole, these results demonstrate that the anti-glycation capacity of *C. paliurus* leaves is strongly dependent on harvest month, with later growth stages, particularly Q9, exhibiting the most pronounced inhibitory effects against AGEs formation. Recent transcriptomic and metabolomic analyses have also identified the late growth stage (September) as a critical period for the biosynthesis of hypoglycemic and functional metabolites in *C. paliurus* [**Error! Reference source not found.**].

3.4. Analysis of VOCs by GC-MS

The volatile organic compounds (VOCs) in *C. paliurus* leaves collected at different growth stages (Q5–Q9) were identified and quantified by GC–MS, and the results are summarized at both class and individual compound levels (Figure 4 and Table 2). A diverse array of volatile constituents, including alkanes, alkenes, aldehydes, alcohols, ketones, and other compounds, was detected, exhibiting pronounced growth-stage-dependent variations in both composition and relative abundance.

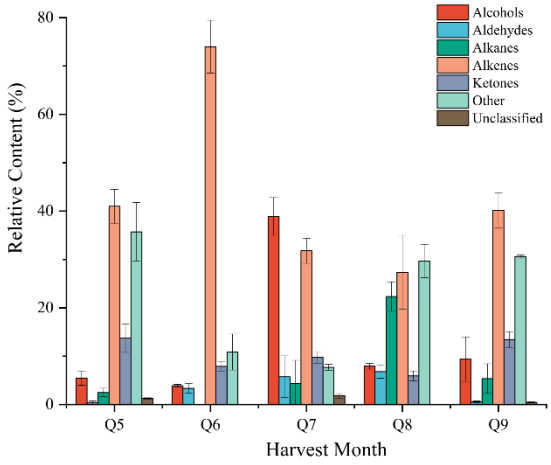

Figure 4. Changes in volatile components of C. paliurus leaves in five different months Note: Q5-Q9 refers to the samples of the leaves of C. paliurus collected from May to September.

Table 2. The composition and content of volatile compounds in the leaves of *C. paliurus* in different months.

class	Compound Name	CAS No.	Q5		Q6		Q7		Q8		Q9	
			Content (%)	RT (min)	Content (%)	RT (min)	Content (%)	RT (min)	Content (%)	RT (min)	Content (%)	RT (min)
Alkanes	Cyclohexene, 4-bromo-	3540-84-9	-	-	1.74	15.86	-	-	1.71	15.83	0.97	15.83
	1-Chloroheptane	629-06-1	-	-	-	-	0.39	14.42	0.32	14.38	-	-
	1-Chlorohexane	544-10-5	-	-	-	-	1.31	8.97	-	-	0.46	8.97
	Tridecane	629-50-5	-	-	-	-	-	-	0.37	40.94	0.18	40.93
	trans-Sabinene hydrate	17699-16-0	-	-	2.52	22.75	-	-	-	-	-	-
	(1S,2R,5S)-2,6,6-trimethylbicyclo [3.1.1]heptane	6876-13-7	-	-	-	-	0.98	17.15	-	-	-	-
	1-Methyl-2-(1-methylpentyl)cyclopropane	62238-06-6	-	-	0.38	14.43	-	-	-	-	-	-
	1-methylene-4-(1-methylvinyl)cyclohexane	499-97-8	-	-	-	-	-	-	-	-	0.50	17.73
	2-methylbutan-2-ylcyclohexane	31797-64-5	-	-	0.90	27.26	-	-	-	-	-	-

 doi:10.20944/preprints202602.1111.v1

	3,9-dimethylundecane	17301-31-4	-	-	-	-	0.45	36.25	-	-	-	-
	3-CHLOROOCTANE	1117-79-9	-	-	4.75	18.01	-	-	-	-	-	-
	3-Methylundecane	1002-43-3	-	-	-	-	-	-	-	-	0.27	31.29
	4-BROMO-1-CYCLOHEXENE	3540-84-9	1.32	15.76	-	-	-	-	-	-	-	-
	4-bromocyclohexene		-	-	-	-	2.17	15.80	-	-	-	-
	Bicyclo[3.1.1]heptane, 2,6,6-trimethyl-, (1R,2R,5R)-rel-	10281-53-5	-	-	-	-	-	-	-	-	0.39	17.18
	Bicyclo[3.2.0]heptane,2-ethenyl-2,6,6-trimethyl-1-(1-methylethenyl)-,(1R,2S,5S)-rel-	871660-95-6	-	-	-	-	-	-	-	-	15.82	40.66
	Bromo-1-chloro		-	-	-	-	-	-	-	-	10.77	5.09
	Cyclodecane	293-96-9	-	-	-	-	1.11	29.00	-	-	-	-
	Cyclooctane, 1,4-dimethyl-, cis-	10565-37-4	-	-	-	-	-	-	3.65	20.73	-	-
	α-Isocomene	65372-78-3	-	-	-	-	1.02	43.83	16.04	43.85	-	-
	2-Chlorooctane	628-61-5	1.46	17.91	-	-	-	-	-	-	-	-
	4-Chlorooctane	999-97-3	-	-	-	-	7.19	17.51	-	-	-	-
	Octylcyclopropane	1472-12-4	-	-	-	-	0.98	24.53	-	-	-	-
	α-Cubebene	17699-14-8	0.96	43.45	1.38	43.45	1.04	43.49	6.18	43.52	-	-
	3-Bromocyclohexene	1521-51-3	1.61	16.62	3.67	16.73	2.04	16.68	3.07	16.68	-	-
	α-ylangene	14912-44-8	45.35	44.79	0.92	44.77	1.88	44.77	-	-	-	-
	Cyclosativene	22469-52-9	-	-	0.39	44.59	-	-	-	-	3.41	44.02
	(Z)-2-Undecene	764-85-2	-	-	1.19	25.71	2.30	25.67	-	-	-	-
	Hydrocarbon C12		-	-	0.98	26.87	3.00	25.92	-	-	-	-
	α-Longipinene	5989-08-2	-	-	0.84	42.73	6.37	43.87	-	-	-	-
	Menthofuran	494-90-6	-	-	-	-	0.75	32.58	1.01	32.60	-	-
	Panaxene	871660-95-6	-	-	-	-	3.12	40.64	15.72	41.55	-	-
	β-Elemene	3388-04-3	-	-	-	-	0.99	45.82	1.21	45.82	-	-
	Viridoflorene	21747-46-6	-	-	-	-	2.36	46.63	0.55	46.63	-	-
	β-Caryophyllene	87-44-5	1.76	47.15	-	-	2.89	47.54	-	-	-	-
	Longifolene	475-20-7	-	-	-	-	3.08	46.36	3.42	46.36	-	-
	β-Longipinene	15301-20-4	-	-	-	-	-	-	-	-	0.67	46.34
	α-Guaiene	3691-12-1	-	-	-	-	12.93	47.97	-	-	-	-
Alkenes	Longicyclene	1137-12-8	-	-	-	-	-	-	-	-	9.47	44.32
	Alloaromadendrene	25246-27-9	-	-	1.97	47.92	-	-	-	-	-	-
	α-Calamenene	483-77-2	-	-	-	-	-	-	2.30	44.77	-	-
	Ascaridole	512-85-6	-	-	0.33	37.84	-	-	-	-	-	-
	trans-Carveol	1197-07-5	-	-	-	-	3.04	35.77	0.83	35.78	0.22	35.75
	8-Methyl-1-decene	13151-34-3	-	-	-	-	2.21	22.14	-	-	-	-
	α-Terpinene	99-86-5	1.22	19.10	-	-	-	-	-	-	-	-
	3-Carene	13466-78-9	-	-	-	-	0.48	19.14	-	-	-	-
	Viridoflorene	21747-46-6	-	-	-	-	-	-	-	-	0.37	47.46
	Longifolene	475-20-7	-	-	-	-	1.22	45.58	-	-	-	-
	Edulan I	41678-25-5	-	-	-	-	2.05	41.40	-	-	-	-
	Valencene	4630-07-3	-	-	-	-	-	-	-	-	0.62	48.51
	Rhodinol	141-25-3	-	-	-	-	-	-	-	-	0.25	33.44
	α-Copaene	3856-25-5	-	-	-	-	-	-	-	-	2.30	44.76
	α-Ylangene	14912-44-8	-	-	-	-	-	-	-	-	0.17	45.01
	β-Copaene	18252-44-3	-	-	-	-	-	-	-	-	0.15	47.39

 doi:10.20944/preprints202602.1111.v1

	α-Patchoulene	560-32-7	-	-	-	-	-	-	9.57	43.95	-	-
	δ -Elemene	20307-84-0	-	-	-	-	-	-	1.60	41.84	-	-
Alkynes	1-Undecyne	2243-98-3	-	-	-	-	4.86	23.08	9.19	23.10	2.71	23.06
	2-Decyne	2384-86-3	1.43	20.69	-	-	-	-	-	-	-	-
	2-Decyne	2384-86-3	-	-	5.14	20.75	-	-	-	-	-	-
Aldehydes	(Z)-6-Nonenal	2277-19-2	-	-	-	-	4.11	24.03	-	-	-	-
	10-Undecenal	112-45-8	-	-	-	-	-	-	0.34	39.69	-	-
	(E)-2-Ethyl-2-butenal	19780-25-7	-	-	-	-	4.35	8.26	-	-	-	-
	2-Ethylhexanal	123-05-7	-	-	-	-	0.74	14.82	-	-	-	-
	(E)-2-Hexenal	6728-26-3	-	-	-	-	-	-	-	-	0.27	8.37
	2-Methyl-2-pentenal	623-36-9	-	-	2.97	8.22	-	-	-	-	-	-
	Hexanal	66-25-1	-	-	1.09	6.38	-	-	-	-	-	-
Alcohols	(E)-2-Nonen-1-ol	31502-14-4	0.97	31.76	-	-	1.48	31.33	1.37	31.79	-	-
	trans-Isopiperitenol	16721-39-4	-	-	0.95	34.11	-	-	0.44	34.12	-	-
	Ocimenol	2270-40-8	-	-	3.12	30.24	1.54	30.24	-	-	-	-
	trans-Carveol	1197-07-5	-	-	-	-	3.04	35.77	0.83	35.78	0.22	35.75
	(-)-Isopulegol	89-79-2	-	-	3.32	29.06	-	-	1.65	29.04	-	-
	cis-p-Mentha-2,8-dien-1-ol	4017-02-1	-	-	-	-	1.84	23.65	-	-	-	-
	3-Thujanol	546-79-2	-	-	-	-	-	-	0.56	27.80	-	-
	cis-Sabinene hydrate	15537-55-0	0.99	22.66	-	-	-	-	-	-	-	-
	β-Terpineol	138-87-4	-	-	-	-	-	-	5.74	30.36	-	-
	cis-Carveol	13429-07-7	-	-	-	-	2.20	34.10	-	-	-	-
	3,3,5-Trimethylcyclohexanol	116-02-9	-	-	5.05	23.10	-	-	-	-	-	-
	3-Methyl-1-heptanol	1470-24-2	-	-	-	-	-	-	-	-	1.05	20.74
	4-Methyl-1-pentanol	626-89-1	-	-	2.67	8.93	-	-	-	-	-	-
	(Z)-Ocimenol	106064-70-0	-	-	-	-	-	-	-	-	4.34	30.23
	Sulcatol	1569-60-4	-	-	0.62	17.15	-	-	-	-	-	-
	Neoisothujanol	21653-20-3	-	-	0.35	31.35	-	-	-	-	-	-
	3-Thujanol	546-79-2	-	-	-	-	0.86	30.91	-	-	-	-
	trans-Verbenol	1820-09-3	-	-	-	-	-	-	0.37	28.81	-	-
	cis-Sabinene hydrate	15537-55-0	-	-	-	-	-	-	-	-	0.52	22.72
	(Z)-2-(3,3-Dimethylcyclohexylidene)ethanol	55253-28-6	-	-	-	-	2.82	36.47	-	-	-	-
	Isopulegol	89-79-2	-	-	-	-	-	-	-	-	2.44	30.25
	Sabinene hydrate	546-87-2	-	-	-	-	-	-	1.03	22.74	-	-
	trans-p-Mentha-2,8-dien-1-ol	3886-78-0	-	-	-	-	-	-	-	-	0.26	26.84
Ketones	6-Methyl-6-hepten-2-one	10408-15-8	2.11	15.22	5.98	15.30	3.40	15.28	1.73	15.33	2.23	15.33
	2-Octyl trifluoroacetate	13109-64-3	-	-	21.54	17.60	-	-	-	-	-	-
	Isolongifolene	1135-66-6	-	-	-	-	-	-	-	-	1.88	42.37
	Isobornyl acetate	125-12-2	-	-	-	-	1.55	32.37	-	-	-	-
	Dihydrojasmone	1128-08-1	-	-	0.23	44.94	-	-	-	-	-	-
	2-Tridecanone	593-08-8	-	-	0.29	51.08	-	-	-	-	-	-
Others	Carbofuran phenol	1563-38-8	-	-	0.40	39.42	1.89	39.41	1.32	39.42	0.82	39.42
	Dill ether	74410-10-9	-	-	-	-	-	-	-	-	0.50	32.57
	Chloroacetyl chloride	79-04-9	-	-	-	-	-	-	-	-	14.18	3.24
	Cyperene	2387-78-2	-	-	-	-	-	-	-	-	0.15	45.16
	Piperitol acetate	5258-29-7	-	-	-	-	0.99	41.83	-	-	-	-
	Neoisothujyl acetate	52673-82-4	-	-	-	-	-	-	4.43	38.60	-	-
	Emylcamate	78-28-4	-	-	0.59	24.56	-	-	-	-	-	-

 doi:10.20944/preprints202602.1111.v1

Isopentylbenzene	2049-94-7	-	-	0.42	23.75	-	-	-	-	-	-
2,8-Dimethylquinoline	1463-17-8	-	-	-	-	-	-	-	-	0.22	45.29
2,5-Di-tert-butyl-1,4-benzoquinone	2460-77-7	-	-	-	-	-	-	-	-	0.25	48.81
EdulanI	41678-25-5	-	-	-	-	-	-	-	-	0.26	41.40

At the compound class level, alkenes predominated among the volatile constituents across most growth stages, with a particularly high relative abundance observed in June (Q6), where they accounted for 74.00% of the total volatiles. In contrast, the volatile profile of early-stage leaves (Q5) exhibited a more heterogeneous composition, characterized by a balanced contribution of alkenes (40.99%), ketones (13.70%), and a substantial proportion of other unclassified compounds (35.70%).

As leaf development progressed, distinct shifts in chemical classes were observed. Alcohols displayed a striking accumulation pattern, showing a sharp peak in July (Q7, 38.90%), suggesting a specific metabolic shift towards hydroxylated compounds during this mid-growth period. Subsequently, alkanes increased markedly in August (Q8), reaching their highest level of 22.32%, before declining in September (Q9). Ketones, on the other hand, exhibited a bimodal distribution, with higher levels observed in the early (Q5, 13.70%) and late (Q9, 13.32%) stages, and lower proportions during the mid-summer months. Notably, the category of "other compounds" remained high in Q5, Q8, and Q9 (approx. 30–35%), indicating a complex accumulation of diverse metabolites during these specific periods.

At the individual compound level (Figure 4 and Table 3), the volatile profiles exhibited substantial qualitative turnover across different growth stages. The high proportion of alkenes observed in Q6 suggests a predominance of terpene hydrocarbons during the rapid vegetative growth phase. In contrast, the pronounced increase in alcohols at Q7 indicates enhanced oxidative modification of volatile precursors, potentially triggered by elevated temperatures or developmentally regulated metabolic shifts in mid-summer. During the late growth stage (Q9), the re-emergence of ketones along with a broader array of other volatile compounds points to further metabolic reprogramming associated with leaf maturation or the onset of senescence. Such dynamic changes in volatile composition, particularly the increasing complexity and differentiation of chemical fingerprints across harvest periods, are widely recognized as important determinants of quality variation in *C. paliurus* [38].

Table 3. Odor descriptions of the aroma components of *C. paliurus* leaves in different months.

month	CAS	Compound	molecular formula	Odor description
Q5	2384-70-5	2-Decyne	$C_{10}H_{18}$	Lemon, medicinal, citrus
	31502-14-4	trans-2-Nonen-1-ol	$C_9H_{18}O$	Waxy, violet
	74410-10-9	Dill ether	$C_{10}H_{16}O$	Dill-like
	17699-14-8	α-Cubebene	$C_{15}H_{24}$	Sweet, herbal, woody
	118-65-0	γ -Muurolene	$C_{15}H_{24}$	Woody, spicy
	87-44-5	β -Caryophyllene	$C_{15}H_{24}$	Sweet, woody, spicy, clove-like
Q6	66-25-1	Hexanal	$C_6H_{12}O$	Pungent
	623-36-9	2-Methyl-2-pentenal	$C_6H_{10}O$	Aldehydic, fruity, garlic-like, ripe cherry, earthy
	626-89-1	4-Methyl-1-pentanol	$C_6H_{14}O$	Nutty
	2384-70-5	2-Decyne	$C_{10}H_{18}$	Lemon, medicinal, citrus
	116-02-9	3,3,5-Trimethylcyclohexanol	$C_9H_{18}O$	Minty, musty, spicy
	89-79-2	(-)-Isopulegol	$C_{10}H_{18}O$	Minty, cooling, medicinal, woody
	17699-14-8	α-Cubebene	$C_{15}H_{24}$	Sweet, herbal, woody
	1128-08-1	Dihydrojasmone	$C_{11}H_{18}O$	Jasmine, myrrh, woody
Q7	13466-78-9	3-Carene	$C_{10}H_{16}$	Citrus, terpenic, medicinal, woody
	31502-14-4	trans-2-Nonen-1-ol	$C_9H_{18}O$	Waxy, violet
	1197-07-5	trans-Carveol	$C_{10}H_{16}O$	Spearmint
	1197-06-4	cis-Carveol	$C_{10}H_{16}O$	Caraway
	17699-14-8	α-Cubebene	$C_{15}H_{24}$	Sweet, herbal, woody
	515-13-9	β -Elemene	$C_{15}H_{24}$	Sweet
	87-44-5	β -Caryophyllene	$C_{15}H_{24}$	Sweet, woody, spicy, clove-like
	3691-12-1	α-Guaiene	$C_{15}H_{24}$	Sweet, woody, balsamic, peppery

 doi:10.20944/preprints202602.1111.v1

Q8	15537-55-0	cis-Sabinene hydrate	$C_{10}H_{18}O$	Balsam-like
	89-79-2	(-)-Isopulegol	$C_{10}H_{18}O$	Minty, cooling, medicinal, woody
	31502-14-4	trans-2-Nonen-1-ol	$C_9H_{18}O$	Waxy, violet
	74410-10-9	Dill ether	$C_{10}H_{16}O$	Dill-like
	1197-06-4	cis-Carveol	$C_{10}H_{16}O$	Caraway
	20307-84-0	δ -Elemene	$C_{15}H_{24}$	Sweet, herbal, woody
	17699-14-8	α-Cubebene	$C_{15}H_{24}$	Sweet, herbal, woody
	515-13-9	β -Elemene	$C_{15}H_{24}$	Sweet
	3691-12-1	α-Guaiene	$C_{15}H_{24}$	Sweet, woody, balsamic, peppery
Q9	979-4-9	Chloroacetyl chloride	C2H2Cl2O	Strong, pungent
	505-57-7	2-Hexenal	C6H10O	Green, leafy, fruity
	3886-78-0	trans-p-Mentha-2,8-dien-1-ol	C10H16O	Fresh, minty
	89-79-2	Isopulegol	C10H18O	Minty, cooling, medicinal, woody
	1002-43-3	3-Methylundecane	C12H26	Mild, waxy
	74410-10-9	Dill ether	C10H16O	Dill-like
	6812-78-8	Rhodinol	C10H20O	Floral
	1197-06-4	cis-Carveol	C10H16O	Caraway
	20307-84-0	δ -Elemene	C15H24	Sweet, herbal, woody
	17699-14-8	α-Cubebene	C15H24	Herbal
	3856-25-5	α-Copaene	$C_{15}H_{24}$	Honey-like
	515-13-9	β -Elemene	$C_{15}H_{24}$	Sweet

The observed shifts in volatile organic compounds (VOCs) composition are consistent with the variations in biological activities. The enrichment of oxygenated volatiles, particularly alcohols at Q7, together with the increased structural diversity of terpenoids, may indirectly contribute to the antioxidant and anti-glycation potential of *C. paliurus* leaves. Although volatile organic compounds are not considered major contributors to radical scavenging activity, their pronounced temporal transitions from hydrocarbon dominated profiles at Q6 to alcohol and alkane enriched compositions at Q7 and Q8 provide important chemical evidence for harvest stage dependent functional differentiation in *C. paliurus* leaves. Similar dynamic shifts in volatile composition, especially involving terpenoids and oxygenated compounds, have been widely recognized as key factors underlying quality differentiation in *C. paliurus* tea [**Error! Reference source not found.**]. In general, the GC–MS analysis demonstrates that the harvest timing significantly influences the volatile signature of *C. paliurus* leaves. These compositional dynamics highlight that June and July are critical periods for the accumulation of terpenoid hydrocarbons and alcohols, respectively, which determines the sensory attributes and potential functional value of the leaf products.

3.5. Correlation Analysis Between Volatile Organic Compounds and Antioxidant and Anti-Glycation Activities of C. paliurus Leaves Collected in Different Months

To further explore the potential relationships between the volatile organic compounds (VOCs) composition variability and biological functions of *C. paliurus* leaves, a hierarchical clustering heatmap was constructed based on the normalized contents of VOC classes, primary metabolites (TP, TSC), secondary metabolites (TPC, TFC), and bioactivities (antioxidant and anti-glycation) (Figure 5). The growth stage dependent clustering observed in the heatmap highlights substantial metabolic and functional divergence of *C. paliurus* leaves across the harvest period.

A striking synchronous accumulation pattern was observed in the late growth stage (Q9). As shown in Figure 5, Q9 was characterized by the highest intensity of Antioxidant Activity (dark red blocks), which clustered tightly with Ketones and Total Protein (TP). This co-occurrence suggests that the specific accumulation of ketone-type volatiles (e.g., potential oxidation products) in September might contribute synergistically to the enhanced radical scavenging capacity, or they may share common biosynthetic regulatory pathways responding to late-season environmental signals.

 doi:10.20944/preprints202602.1111.v1

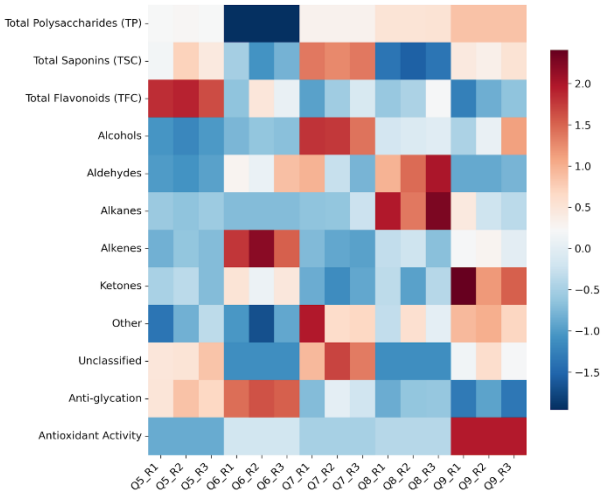

Figure 5. The relative composition of major volatile compound classes of C. paliurus leaves at different growth stages. Note: Q5-Q9 refers to the samples of the leaves of C. paliurus collected from May to September.

In contrast, Anti-glycation activity displayed a different temporal profile, showing relatively higher levels in the mid-growth stages (Q6–Q7). This activity pattern aligned closely with the high relative abundance of Alkenes and Total Flavonoids (TFC) observed in Q6. Notably, although Total Phenols (TPC) were most abundant in the early stage (Q5), their decline in subsequent months did not strictly parallel the trends in bioactivities, implying that specific phytochemical classes (such as flavonoids or specific volatile terpenes) might be more biologically relevant contributors than the total phenolic pool in this context. This complex relationship reflects the metabolic network reprogramming that occurs during leaf maturation, as revealed by joint transcriptomic and metabolic analyses [**Error! Reference source not found.**].

Furthermore, aldehydes and alkanes formed a distinct cluster with maximal abundance at Q8 and exhibited a comparatively weaker association with the evaluated bioactivities than other classes of volatile organic compounds. Overall, the correlation analysis indicates that the functional properties of *C. paliurus* leaves are not governed by a single class of constituents but instead arise from complex interactions between the non-volatile matrix (notably flavonoids) and specific volatile signatures, such as ketones and alkenes, which dynamically shift during leaf maturation.

3.6. Characterization of Key Aroma-Active Compounds and Sensory Profiles

Beyond the functional bioactivities revealed by the correlation analysis, the variation in volatile composition profoundly influences the sensory quality of *C. paliurus* leaves, which is a decisive factor for consumer acceptance. While the heatmap (Figure 4) highlighted the quantitative shifts of chemical classes, Table 3 provides a detailed qualitative insight into the specific odor-active compounds responsible for the unique aroma profiles across different harvest months.

In the early growth stage (Q5), the aroma profile was predominantly characterized by woody, herbal, and spicy notes, largely attributed to the accumulation of sesquiterpenes. Key contributors includedα-Cubebene (sweet, herbal, woody), γ-Muurolene (woody, spicy), and β-Caryophyllene (clove-like, spicy). The presence of Dill ether introduced a characteristic herbal nuance, while 2-Decyne added a medicinal, citrusy background. This suggests that early-season leaves possess a robust, medicinal sensory character typical of herbal teas.

A dramatic sensory shift occurred in June (Q6), transitioning towards a fresher, fruitier, and more floral profile. This stage was distinguished by the emergence of aldehydes and oxygenated compounds such as Hexanal (pungent) and 2-Methyl-2-pentenal (fruity, ripe cherry-like), which impart the "green" freshness associated with young leaves. Notably, the detection of (-)-Isopulegol (minty, cooling) and Dihydrojasmone (jasmine, woody) indicates a significant enrichment in cooling

 doi:10.20944/preprints202602.1111.v1

and floral attributes, making Q6 a critical period for harvesting leaves with refreshing sensory qualities.

During the mid-to-late summer stages (Q7 and Q8), the volatile signature evolved to feature sweet, balsamic, and minty characteristics. The appearance of trans/cis-Carveol contributed distinct spearmint and caraway notes. Furthermore, sesquiterpenes such as β-Elemene andδ-Elemene provided sweet undertones, while α-Guaiene offered a unique balsamic and peppery aroma. cis-Sabinene hydrate in Q8 further reinforced the balsamic profile, suggesting that leaves harvested in July and August develop a mellower, richer fragrance compared to the sharp freshness of June.

In the late growth stage (Q9, September), the aroma profile became highly complex, blending green, floral, and honey-like notes. The re-emergence of green leaf volatiles like 2-Hexenal (green, leafy, fruity) alongside Rhodinol (floral, rose-like) and α-Copaene (honey-like) created a unique sensory phenotype. Although some waxy alkanes (e.g., 3-Methylundecane) were detected, the persistence of sweet and floral modulators indicates that late-harvest leaves still retain desirable aroma properties, potentially suitable for specific tea product formulations requiring a heavy, sweet fragrance.

Collectively, the odor activity analysis reveals a distinct temporal succession of aroma types: from the Herbal/Woody dominance in May, to the Fresh/Floral/Minty peak in June, followed by Sweet/Balsamic notes in July–August, and finally a Green/Honey-like profile in September. These findings provide a scientific basis for precision harvesting: Q6 is optimal for producing fresh-scented beverages, while Q5 and Q7–Q8 may be better suited for functional teas with medicinal or rich balsamic characteristics. This approach is supported by the identification of specific taste-active compounds that fluctuate seasonally, directly influencing the flavor profile and consumer acceptance of *C. paliurus* product [1,38].

4. Discussion

Based on the temporal dynamics of volatile metabolic signatures and their correlations with bioactivities, a schematic model was proposed to illustrate the seasonal functional divergence of *C. paliurus* leaves (Figure 6). This conceptual framework divides the harvest period into three distinct physiological phases characterized by coordinated shifts in metabolism and biological function.

Phase I (Summer growth phase, Q5–Q7) is marked by a pronounced biosynthetic activation of secondary metabolites, particularly terpenoid hydrocarbons (alkenes) and flavonoids. As illustrated in Fig. 6, anti-glycation activity closely parallels the accumulation of alkenes, reaching its maximum in June (Q6). This synchrony suggests that the vigorous secondary metabolism associated with rapid leaf expansion primarily contributes to the glycation-inhibitory potential of the leaves during early and mid-summer.

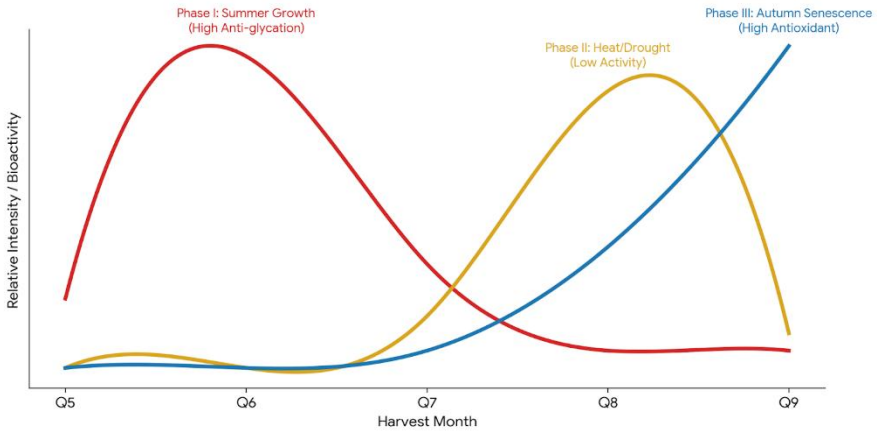

 doi:10.20944/preprints202602.1111.v1

Figure 6. Proposed mechanism linking volatile metabolic dynamics to the temporal separation of antioxidant and anti-glycation activities. Note: Q5-Q9 refers to the samples of the leaves of C. paliurus collected from May to September.

Phase II (Stress-response transition phase, Q8) represents a metabolic inflection point occurring in August. During this stage, a distinct enrichment of alkanes is observed (yellow curve in Figure 6), likely reflecting an adaptive response to late-summer heat or drought stress. Increased alkane production is commonly associated with enhanced cuticular wax biosynthesis, which serves to reduce transpirational water loss. Notably, both antioxidant and anti-glycation activities are comparatively reduced during this transitional phase, indicating a temporary shift in metabolic prioritization toward structural protection rather than bioactivity-related functions.

Phase III (Autumn senescence phase, Q9) is characterized by senescence-associated oxidative metabolism. As shown in Fig. 6, the volatile profile shifts toward oxygenated compounds, particularly ketones (blue curve), which are typically derived from fatty acid or terpene oxidation. This phase coincides with a marked increase in total phenolics content and antioxidant capacity. Such synchronization suggests that oxidative stress accompanying senescence induces compensatory upregulation of antioxidant enzymes, ultimately resulting in the highest radical scavenging activity observed at Q9.

Collectively, this model demonstrates that the functional value of *C. paliurus* leaves is not static but dynamically regulated by developmental progression and environmental cues. The temporal separation of anti-glycation and antioxidant activities provides a mechanistic basis for precision harvesting strategies tailored to specific functional targets.

5. Conclusions

This study systematically elucidates the month-dependent variations of volatile organic compounds (VOCs) and bioactivities in *C. paliurus* leaves from May to September. Our results reveal a distinct harvest-stage dependence: September (Q9) and June (Q6) emerged as peak periods for antioxidant and anti-glycation potential, with Q9 exhibiting the highest DPPH scavenging (IC_{50} = 0.119 mg/mL) and >70% inhibition of advanced glycation end-products (AGEs). The volatile profile underwent significant remodeling, transitioning from alkene predominance in Q6 (74.00%) to alcohol enrichment in July (38.90%). Correlation analysis demonstrates that these functional properties are not driven by isolated compounds, but by a dynamic synergy between the non-volatile matrix (flavonoids) and stage-specific VOCs (alkenes and ketones). We propose a three-phase schematic model where anti-glycation capacity aligns with summer terpenoid enrichment, while antioxidant activity peaks during late-season metabolic shifts. These findings provide a precision-harvesting framework to optimize *C. paliurus* for functional tea production, balancing bioactivity with aroma. Future research will target the molecular coupling mechanisms between bioactive and volatiles to validate these metabolic markers across diverse environments. We hope to report more about these advancements in the future.

Author Contributions: Yanmeng Fu: Conceptualization, Methodology, Formal analysis, Investigation, Writing - original draft, Writing - review & editing. Qiyue Shao: Conceptualization, Formal analysis, Investigation, Writing - original draft. Liang Chen: Formal analysis, Investigation, Writing - original draft. Tianxiao Zhang: Methodology, Data curation, Investigation. Jingyi Zhao: Formal analysis, Investigation. Wenhui Zhou: Methodology, Data curation. Bin Long: Methodology, Conceptualization, Data curation. Dai Lu: Methodology, Formal analysis, Data analysis. Wei Wang: Supervision, Writing - review & editing, Funding acquisition. Xing Tian: Supervision, Writing - review & editing, Funding acquisition.

Acknowledgments: This study was supported by "Hunan Natural Science Foundation Program" (Project No. 2023JJ30445, 2024JJ6337), "Hunan Province Traditional Chinese Medicine Research Project" (Project No. B2024012), The State-sponsored Postdoctoral Researcher Program of China (Project No. GZB20230206). The

 doi:10.20944/preprints202602.1111.v1

authors thank Hunan Yueling Junshan Agriculture and Forestry Technology Co., Ltd. providing the Cyclocarya paliurus leave raw materials support.

Conflicts of Interest: The authors declare that they have no known competing financial interests or personal relationships that could have appeared to influence the work reported in this paper.

References

1. Chen, L.; Lu, D.; Wan, Y.; Zou, Y.; Zhang, R.; Zhou, T.; Long, B.; Zhu, K.; Wang, W.; Tian, X. Metabolite Profiling and Identification of Sweet/Bitter Taste Compounds in the Growth of *Cyclocarya Paliurus* Leaves Using Multiplatform Metabolomics. *Foods*. **2024**, *13*, 3089. [https://doi.org/10.3390/foods13193089]
2. Fang, S.; Sun, D.; Shang, X.; Fu, X.; Yang, W. Variation in radial growth and wood density of *Cyclocarya paliurus* across its natural distribution. *New Forests*. **2020**, *51*, 453-467. [https://doi.org/10.1007/s11056 -019-09742-9]
3. Xie, J.; Wang, Z.; Shen, M.; Nie, S.; Gong, B.; Li, H.; Zhao, Q.; Li, W.; Xie, M. Sulfated modification, characterization and antioxidant activities of polysaccharide from *Cyclocarya paliurus. Food Hydrocolloids: A Key to Human Health Food Hydrocolloids*. **2016**, *53*, 7-15. [https://doi.org/10.1016/j.foodhyd.2015.02.018]
4. Wang, J.; Wang, K. Fatigue-alleviating effect of polysaccharides from *Cyclocarya paliurus* (Batal) Iljinskaja in mice. *Afr J Microbiol Res.* **2012**, *6*, 5243–5248. [https://doi.org/10.5897/AJMR12.655]
5. Wu, Z.; Gao, T.; Zhong, R.; Lin, Z.; Jiang, C.; Ouyang, S.; Zhao, M.; Che, C.; Zhang, J.; Yin, Z. Antihyperlipidaemic effect of triterpenic acid-enriched fraction from *Cyclocarya paliurus* leaves in hyperlipidaemic rats. *Pharm Biol*. **2017**, *55*, 712-721. [https://doi.org/10.1080/13880209.2016.126723110. 1080/13880209.2016.1267231]
6. Shen, Y.; Peng, Y.; Zhu, X.; Li, H.; Zhang, L.; Kong, F.; Wang, J.; Yu, D. The phytochemicals and health benefits of *Cyclocarya paliurus* (Batalin) Iljinskaja. *Front. Nutr*. **2023**, *10*, 1158158. [https://doi.org/10.3389/fnut.2023.1158158]
7. Zhang, J.; Shen, Q.; Lu, J.; Li, J.; Liu, W.; Yang, J.; Li, J.; Xiao, K. Phenolic compounds from the leaves of *Cyclocarya paliurus* (Batal.) Ijinskaja and their inhibitory activity against PTP1B. *Food Chem.* **2010**, *119*, 1491-1496. [https://doi.org/10.1016/j.foodchem.2009.09.031]
8. Wang, Y.; Ma, J.; Tong, Y.; Li, N.; Li, J.; Qi, Z. Antidiabetic effects and mechanisms of *Cyclocarya paliurus* leaf flavonoids via PIK3CA. *J. Funct. Foods.* **2024**, *113*, 106031. [https://doi.org/10.1016/j.jff.2024.106031]
9. Zhou, M.; Lin, Y.; Fang, S.; Liu, Y.; Shang, X. Phytochemical content and antioxidant activity in aqueous extracts of *Cyclocarya paliurus* leaves collected from different populations. *PeerJ.* **2019**, *7*, e6492. [https://doi.org/10.7717/peerj.6492]
10. Dong, Y.; Wang, Z.; Xia, Q.; Chen, J.; Lv, Q.; Zhang, S.; Cheng, S.; Chen, X.; Dong, X. X. Preparation, Structural Characterization and Biological Activity Study of Selenium-Rich Polysaccharides from *Cyclocarya paliurus*. *Foods*. **2025**, *14*, 1641. [https://doi.org/10.3390/foods14091641]
11. Wang, Y.; Zheng, X.; Li, L.; Wang, H.; Wu, H.; Chen, K.; Xu, M.; Wu, Y.; Huang, X. *Cyclocarya paliurus* ethanol leaf extracts protect against diabetic cardiomyopathy in db/db mice via regulating PI3K/Akt/NF-κB signaling. *Food Nutr. Res.* **2020**, *64*, 4267. [https://doi.org/10.4103/1995-7645.273573]
12. Fang, S.; Liu, J.; Wu, C.; Zhang, X.; Dong, H.; Zhang, D.; Hu, C.; Zhang, J.; Pan, K.; Yin, Z.; Qin, Y.; Wang, L. Terpene and lignan glycosides from the leaves of *Cyclocarya paliurus* and their anti-inflammatory activity. *Phytochemistry*. **2025**, *234*, 114443. [https://doi.org/10.1016 /j.phytochem. 2025.114443]
13. Feng,Z.; Fang, Z.; Chen, C.; Vong, C.T.; Chen, J.; Lou, R.; Hoi, M.P.M.; Gan, L.; Lin, L. Anti-hyperglycemic effects of refined fractions from *Cyclocarya paliurus* leaves on streptozotocin-induced diabetic mice. *Molecules*. **2021**, *26*, 6886. [https://doi.org/10.3390/molecules26226886]
14. Xiao, H.; Wen, B.; Ning, Z.; Zhai, L.; Liao, C.; Lin, C.; Mu, H.; Bian, Z. *Cyclocarya paliurus* tea leaves enhances pancreatic β cell preservation through inhibition of apoptosis. *Sci. Rep.* **2017**, *100*, 51-64. [https://doi.org/ 10.1038/s41598-017-09641-z]
15. Zhao, L.; Zhang, Y.; Liu, G.; Deng, Y.; Wang, A.; Ren, F. Effect of *Cyclocarya paliurus* on hypoglycemic effect in type 2 diabetic mice. *Med. Sci. Monit.* **2019**, *25*, 2976–2983. [https://doi.org/10.12659/MSM.913368]

 doi:10.20944/preprints202602.1111.v1

16. Liu, Y.; Cao, Y.; Fang, S.; Wang, T.; Yin, Z.; Shang, X.; Fu, X. Antidiabetic effect of *Cyclocarya paliurus* leaves depends on the contents of antihyperglycemic flavonoids and antihyperlipidemic triterpenoids. *Molecules*. **2018**, *23*, 1420. [https://doi.org/10.3390/molecules23061420]
17. Wang, X.; Li, W.; Kong, D. *Cyclocarya paliurus* extract alleviates diabetic nephropathy by inhibiting oxidative stress and aldose reductase. *Ren. Fail.*. **2016**, *38*, 678-685. [https://doi.org/10.3109/ 0886 022X.2016.1155394]
18. Liang, L.; Zhang, X.; Zhou, Y.; Liu, Y.; Gan, S.; Liu, Y.; Lu, Y.; Lam, H.; Pi, E. Untargeted metabolomics analysis based on HS-SPME-GC-MS and UPLC-Q-TOF/MS reveals the contribution of stem to the flavor of *Cyclocarya paliurus* herbal extract. *LWT*. **2022**, *163*, 113549. [https://doi.org/10.1016/j.lwt.2022.113549]
19. Lou, J.; Zou, Y.; Tian, X. Characterization and analysis of the volatile components of *Cyclocarya paliurus* tea from different origins based on GC-IMS technology. *Food Mach.*. **2024**, *40*, 161-167. (In Chinese) [https://doi.org/ 10.13652/j.spjx.1003.5788.2023.81014]
20. Chen, W.; Zhong, P.; Wang, Y. Analysis of volatile components in *Cyclocarya paliurus* leaves by solid-phase microextraction coupled with gas chromatography-mass spectrometry. *Food Sci*. **2016**, *37*, 136-140. (In Chinese) [https://doi.org/10.7506/spkx1002-6630-201602024]
21. Zheng, X.; Zhang, M.; Qiao, Y.; Li, R.; Alkan, N.; Chen, J.; Chen, F.. *Cyclocarya paliurus* Reprograms the Flavonoid Biosynthesis Pathway Against Colletotrichum fructicola. Front. *Plant Sci.*. **2022**, *13*, 933484. [https://doi.org/10.3389/fpls.2022.933484]
22. Xiao, Y.; He, C.; Chen, Y.; Ho, C.; Wu, X.; Huang, Y.; Gao, Y.; Hou, A.; Li, Z.; Wang, Y.; et al. UPLC–QQQ–MS/MS-based widely targeted metabolomic analysis reveals the effect of solid-state fermentation with *Eurotium cristatum* on the dynamic changes in the metabolite profile of dark tea. *Food Chem*. **2022**, *378*, 131999. [https://doi.org/10.1016/j.foodchem.2021.131999]
23. Yang, J.; Guo, J.; Yuan, J. In vitro antioxidant properties of rutin. *LWT-Food Sci. Technol*. **2008**, *41*, 1060–1066. [https://doi.org/10.1016/j.lwt.2007.06.010]
24. Wu, L.; Gao, Y.; Ren, W.; Su, Y.; Li, J.; Du, Y.; Wang, Q.; Kuang, H. Rapid determination and origin identification of total polysaccharides contents in Schisandra chinensis by near-infrared spectroscopy. *Spectrochim Acta A Mol Biomol Spectrosc*. **2022**, *264*, 120327. [https://doi.org/10.1016/j.saa.2021.120327]
25. Biswas, T.; Dwivedi, U.N. Plant triterpenoid saponins: biosynthesis, in vitro production, and pharmacological relevance. *Protoplasma*. **2019**, *25*, 1463-1486. [https://doi.org/10.1007/s00709-019-01411-0]
26. Svečnjak, L.; Marijanović, Z.; Okińczyc, P.; Marek Kuś, P.; Jerković, I. Mediterranean Propolis from the Adriatic Sea Islands as a Source of Natural Antioxidants: Comprehensive Chemical Biodiversity Determined by GC-MS, FTIR-ATR, UHPLC-DAD-QqTOF-MS, DPPH and FRAP Assay. *Antioxidants*. **2020**, *9*, 337. [https://doi.org/10.3390/antiox9040337]
27. Hasan, M.; Haque, M.; Hoque, M.; et al. Antioxidant activity study and GC-MS profiling of *Camellia sinensis* Linn. *Heliyon*. **2024**, *10*, e23514. [https://doi.org/10.1016/j.heliyon.2023.e23514]
28. Zhou, Q.; Liang, W.; Wan, J.; Wang, M. Spinach (Spinacia oleracea) microgreen prevents the formation of advanced glycation end products in model systems and breads. *Curr. Res. Food Sci.* **2023**, *6*, 100490. [https://doi.org/10.1016/j.crfs.2023.100490]
29. Fu, Y.; Zou, Y.; Tian, X. Analysis of flavor characteristics and bioactive components of *Cyclocarya paliurus* tea from different origins based on electronic tongue and HS-SPME-GC-MS technology. *Sci. Technol. Food Ind*. **2025**, 1-21. (In Chinese) [https://doi.org/10.13386/j.issn1002-0306.2025070013]
30. Cao, Y.; Fang, S.; Fu, X.; Shang, X.; Yang, W. Seasonal variation in phenolic compounds and antioxidant activity in leaves of *Cyclocarya paliurus* (Batal.) Iljinskaja. *Forests*. **2019**, *10*, 624. [https://doi.org/10.3390/f10080624]
31. Zheng, X.; Xiao, H.; Chen, J.; Zhu J.; Fu, Y.; Ouyang, S.; Chen, Y.; Chen, D.; Su, J.; Xue, T. Metabolome and whole-transcriptome analyses reveal the molecular mechanisms underlying hypoglycemic nutrient metabolites biosynthesis in *Cyclocarya paliurus* leaves during different harvest stages. *Front. Nutr*. **2022**, *9*, 851569. [https://doi.org/10.3389/fnut.2022.851569]
32. Fu, X.; Zhou, X.; Deng, B.; Liu, F.; Shang, X.; Fang, S. Seasonal and genotypic variation of water-soluble polysaccharide content in leaves of *Cyclocarya paliurus*. *South. Forests*. **2015**, *77*, 231–275. [https://doi.org/10.2989/20702620.2015.1010698]

 doi:10.20944/preprints202602.1111.v1

33. Fang, S.; Yang, W.; Chu, X.; Shang, X.; She, C.; Fu, X. Provenance and temporal variations in selected flavonoids in leaves of *Cyclocarya paliurus*. *Food Chem.* **2011**, *124*, 1382–1386. [https://doi.org/10.1016/j.foodchem.2010.07.095]
34. Sheng, X.; Chen, H.; Wang, J.; Zheng, Y.; Li, Y.; Jin, Z. Joint Transcriptomic and Metabolic Analysis of Flavonoids in *Cyclocarya paliurus* Leaves. *ACS Omega* **2021**, *6*, 8272-8282. [https://doi.org/10.1021/acsomega.1c00059]
35. Lin, W.; Li, Y.; Lu, Q.; Lu, H.; Li, J. Combined Analysis of the Metabolome and Transcriptome Identified Candidate Genes Involved in Phenolic Acid Biosynthesis in the Leaves of *Cyclocarya paliurus*. *Int. J. Mol. Sci*. **2020**, *21*, 1337. [https://doi.org/10.3390/ijms21041337]
36. Lin, W.; Chen, H.; Wang, J.; Zheng, Y.; Lu, Q.; Zhu, Z.; Li, N.; Jin, Z.; Li, J.; Lu, H. Transcriptome analysis associated with polysaccharide synthesis and their antioxidant activity in *Cyclocarya paliurus* leaves of different developmental stages. *PeerJ*. **2021**, *9*, e11615. [https://doi.org/10.7717/peerj.11615]
37. Xia, X.; Xue, S.; Song, G.; Li, B.; Wang, H.; Qiu, J.; Wang, J.; Liu, Q.; Ma, Y.; Ouyang, J. Antioxidative and immunological role of *Cyclocarya paliurus* polysaccharide in diabetic rats.*J. Tradit. Chin. Med*. **2021**, *41*(6), 739–746. [https://doi.org/10.19852/j.cnki.jtcm.2024.06.005]
38. Cao, Y.; Fang, S.; Yin, Z.; Fu, X.; Shang, X.; Yang, W.; Yang, H. Chemical fingerprint and multicomponent quantitative analysis for the quality evaluation of *Cyclocarya paliurus* leaves by HPLC-Q-TOF-MS. *Molecules*. **2017**, *22*, 1927. [https://doi.org/10.3390/molecules22111927]
39. Bai, M.; Wang, L. Untargeted metabolomics analysis reveals the effect of fixation on the profile of volatile compounds of *Cyclocarya paliurus* tea. *Pol. J. Food Nutr. Sci*. **2022**, *74*, 333-345. [https://doi.org/10.31883/pjfns/191754]